



***Ab initio* Study of Formation and Structure of Double Diels-Alder Cycloadduct Derived from Sequential Pericyclic Reactions of 2-Pyrone with Cycloocta-1,5-diene**

Tamaki Jikyo, Masashi Eto and Kazunobu Harano*

Faculty of Pharmaceutical Sciences, Kumamoto University, 5-1 Oe-honmachi, Kumamoto 862, Japan

(E-mail: harano@gpo.kumamoto-u.ac.jp)

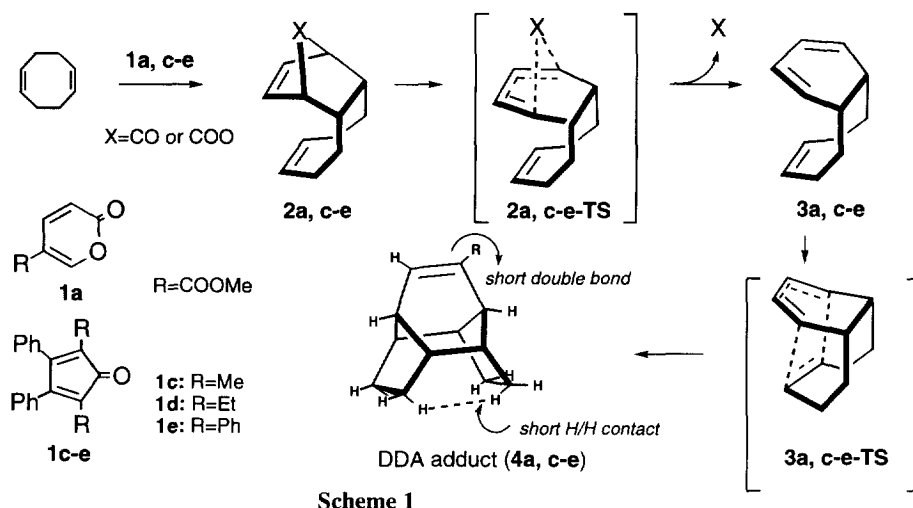
Abstract: Molecular orbital calculations were carried out to interpret the reaction behavior of the formation reaction and structural feature of double Diels-Alder (DDA) adduct derived from three-step sequential pericyclic reactions of 2-pyrone with cycloocta-1,5-diene. The experimental results are correctly predicted by the *ab initio* calculations at the 3-21G level. © 1997 Elsevier Science Ltd.

It has recently become possible to calculate the details of transition-state geometries and energetics by *ab initio* quantum mechanics rather than the approximate descriptions deduced from experimental data. However, although the prototype pericyclic reaction has been studied extensively, there have been relatively few theoretical investigations of pericyclic reactions close to actual reaction systems. As pericyclic reactions include quite a range of reaction types, it might be supposed that the reaction behaviors would vary very widely, depending upon the presence of hetero atoms, the mode of reaction (inter- or intramolecular) and the effects of aromaticity and strain. The RHF/3-21G geometries are quite good for hydrocarbon transition structures. A systematic investigation of the effects of the basis set reveals that the 3-21G results are in reasonable agreement with higher level RHF calculations. In molecules with hetero atoms, calculations with the 6-31G* basis set are necessary to achieve the reliability achieved by the 3-21G basis set for hydrocarbons.¹

In the course of the study on the sequential pericyclic reactions,² we found that the reaction of cyclopentadienones or 2-pyrones with cycloocta-1,5-diene (COD) gave the DDA adduct (**4**) via three-step sequential pericyclic reactions [addends → DA adduct (**2**) → decarboxylated DA adduct (**3**) → DDA adduct (**4**)]. These reactions, the intermediates and the products are suitable targets of *ab initio* calculation because the reactions are remarkably accelerated by the structural features and the X-ray analysis^{2d} of the DDA adduct showed the presence of very close C/C and H/H contacts which were calculated to be considerably shorter than the X-ray and MM3^{3d} values by the semi-empirical SCF MO calculations (AM1^{3a} and PM3^{3b}).

Based on these backgrounds, we performed *ab initio* MO calculations at several levels on the formation reactions and structure of the DDA adduct to explore the best theoretical representation of some different pericyclic reactions with the view to finding the inexpensive computational method that could be reasonably expected to give correct predictions of the reaction behaviors.

This paper describes the overall character of the pericyclic reactions and structural feature of the DDA adducts based on the newly obtained data.



Scheme 1

EXPERIMENTAL

Melting points were uncorrected. The IR spectra were taken with a Hitachi 270-30 spectrophotometer. ¹H-NMR and ¹³C-NMR spectra were taken with JEOL GX-400 spectrometer for *ca.* 10% solution with TMS as an internal standard; chemical shifts are expressed as δ values and the coupling constants (J) are expressed in Hz.

Materials 2,5-dimethyl-3,4-diphenylcyclopentadienone^{4a} (**1c**), 2,5-diethyl-3,4-diphenylcyclopentadienone^{4a} (**1d**) and tetracyclone^{4b} (**1e**) were prepared according to the previously reported methods.

DDA Adduct (4a) of methyl coumalate (1a) and COD

The DDA adduct (**4a**) was prepared according to the previously reported method.^{2c}

DDA Adduct (4b) of methyl coumalate (1a) and 1,5-hexadiene

The DDA adduct (**4b**) was prepared according to the previously reported method.^{2c}

Formation of DDA Adduct (4) (General Procedure)

A mixture of **1c** (1.3 g, 5 mmol) and COD (5.4 g, 50 mmol) was heated at 200° for 44 h in a sealed tube. The excess COD was evaporated off under reduced pressure. The residue was purified by chromatography on silica gel to give **4c**. The solid was recrystallized from ethanol to give colorless needles.

The following compounds were obtained by essentially the same procedure as above.

4c: mp 166-167°; yield 31 %; ¹H-NMR (400 MHz, CDCl₃): δ 7.25-6.86 (10H, m, aromatic H), 1.93-1.90 (4H, d, methylene, $J=9.16$ Hz), 1.72-1.70 (4H, d, methylene, $J=9.89$ Hz), 1.79 (4H, s, methine), 0.91 (6H, s, methyl); ¹³C-NMR (125 MHz, CDCl₃): δ 23.0 (methyl), 24.9 (methylene), 45.6 (quaternary carbon), 47.4 (methine), 125.1, 126.9 and 130.0 (aromatic CH), 141.9 and 142.1 (quaternary carbon); Anal. Calcd for C₂₆H₂₈: C, 91.71; H, 8.29. Found: C, 91.88; H, 8.30.

4d: mp 158-159°; yield 20 %; ¹H-NMR (400 MHz, CDCl₃): δ 7.26-6.85 (10H, m, aromatic H), 1.95-1.90 (8H, m, methylene and methine), 1.67-1.65 (4H, d, methylene, $J=9.68$ Hz), 1.57 (4H, q, methylene, $J=7.32$ Hz), 0.46 (6H, t, methyl, $J=7.32$ Hz); ¹³C-NMR (125 MHz, CDCl₃): δ 9.44 (methyl), 25.0 (-CH₂-CH₃), 25.4 (methylene), 44.8 (methine), 49.4 (quaternary carbon), 124.9, 126.3 and 130.9 (aromatic CH), 141.7 and 142.9 (quaternary carbon); Anal. Calcd for C₂₈H₃₂: C, 91.25; H, 8.75. Found: C, 91.32; H, 8.77.

4e: The DDA adduct (**3e**) was prepared according to the previously reported method.⁵

CALCULATION

Semi-empirical MO calculations were run through the ANCHOR II interface using MOPAC6.0^{3c} on a Fujitsu S4/2 work station (WS). The *ab initio* computations,⁶ running on a S4/10 WS or a Convex Exemplar SPP-1000 parallel computer were carried out using 3-21G and 6-31G basis sets and gradient technique with

Table 1a. Energetics of the Ground-state and Transition-state Structures for the DDA Adduct Formation Reaction.

Geometry	Method	ΔH_f^a	E^b
<u>Reaction of 2-pyrone with COD</u>			
DA adduct (2A)	AM1	-50.28	
	PM3	-45.00	
	RHF/3-21G		-647.6619
TS for Decarboxylation (2A-TS)	AM1	-1.25	
	PM3	5.50	
	RHF/3-21G		-647.5782
Decarboxylated DA adduct (3A)	AM1	30.78	
	PM3	36.94	
	RHF/3-21G		-461.0949
TS for IMDA reaction (3A-TS)	AM1	61.74	
	PM3	67.58	
	RHF/3-21G		-461.0501
DDA adduct (4A)	AM1	15.65	
	PM3	13.74	
	RHF/STO-3G		-458.2633
	RHF/3-21G		-461.1515
	MP2/3-21G		-462.2319
	RHF/6-31G		-463.5147
	MP2/6-31G		-464.5983
	RHF/6-31G*		-463.7022
	MP2/6-31G*		-465.2672
<u>Reaction of 2-pyrone with ethylene</u>			
DA adduct of 2-pyrone and ethylene (2Z)	AM1	-61.35	
	PM3	-62.73	
	RHF/3-21G		-417.1179
	RHF/6-31G**/3-21G		-419.4482
	MP2/6-31G**/3-21G		-420.6931
TS for Decarboxylation (2Z-TS)	AM1	-14.25	
	PM3	-10.99	
	RHF/3-21G		-417.0314
	RHF/6-31G**/3-21G		-419.3687
	MP2/6-31G**/3-21G		-420.6329
<u>Reaction of 2-pyrone with 1,5-hexadiene</u>			
6-(3-butenyl)-1,3-cyclohexadiene (3B)	AM1	26.86	
	PM3	31.03	
	RHF/3-21G		-384.6264
	RHF/6-31G**/3-21G		-386.7715
	MP2/6-31G**/3-21G		-388.0471
TS for IMDA reaction (3B-TS)	AM1	58.73	
	PM3	66.12	
	RHF/3-21G		-384.5720
	RHF/6-31G**/3-21G		-386.6995
	MP2/6-31G**/3-21G		-388.0233

a) Kcal/mol. b) Hartree.

optimization of all variables. The stationary points calculated for the transition states of the decarboxylation and intramolecular Diels-Alder (IMDA) reactions by PM3 method were used as starting geometries. We characterized the stationary point for the synchronous mechanism as a true transition state having a single negative Hessian eigenvalue. Graphic analysis of the MO calculation data was performed on a Macintosh 8500/166 personal computer.

The calculated ground-state (GS) and transition-state (TS) energies for two parent DDA formation reactions [the formation reaction of the DDA adduct (**4A**) of 2-pyrone and COD: **2A** → **2A-TS** → **3A** → **3A-TS** → **4A** and the IMDA reaction of the DA adduct (**3B**) of 2-pyrone and 1,5-hexadiene: **3B** → **3B-TS**] and a model reaction [the decarboxylation reaction of the DA adduct (**2Z**) of 2-pyrone and ethylene: **2Z** → **2Z-TS**] are listed in Table 1a.

The reaction barriers of the parent reactions were estimated from the energy differences between the ground state and transition state, which are listed in Table 1b.

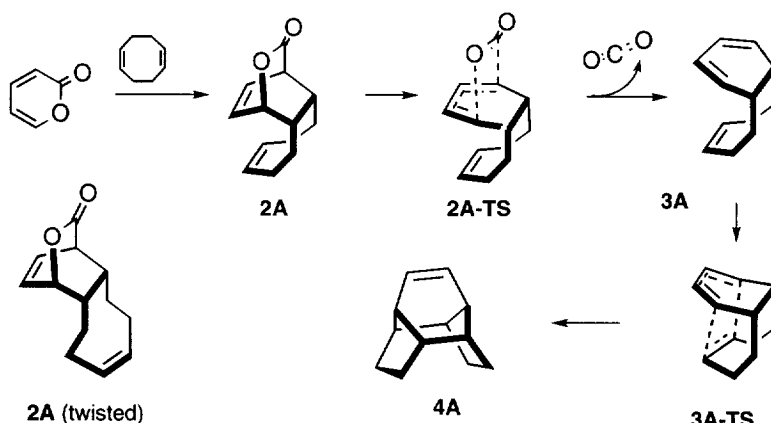


Table 1b. Reaction Barriers for Decarboxylation and IMDA reactions in the DDA Adduct Formation Reaction.

Reaction calculated	Method	$\Delta\Delta H^{\ddagger(a)}$	$\Delta\Delta E^{\ddagger(a)}$
<u>Reaction of 2-pyrone with COD</u>			
Decarboxylation (2A → 2A-TS)	AM1	49.03	
	PM3	50.50	
IMDA reaction (3A → 3A-TS)	RHF/3-21G		52.49
	AM1	30.96	
	PM3	30.64	
	RHF/3-21G		28.11
<u>Reaction of 2-pyrone with ethylene</u>			
Decarboxylation (2Z → 2Z-TS)	AM1	47.10	
	PM3	51.74	
	RHF/3-21G		54.28
	RHF/6-31G**/3-21G		49.94
	MP2/6-31G**/3-21G		37.73
<u>Reaction of 2-pyrone with 1,5-hexadiene</u>			
IMDA reaction (3B → 3B-TS)	AM1	31.87	
	PM3	35.09	
	RHF/3-21G		34.11
	RHF/6-31G**/3-21G		45.21
	MP2/6-31G**/3-21G		14.93

a) Kcal/mol.

RESULTS AND DISCUSSION

Transition Structure of Decarboxylation

The 3-21G GS (**2A**) and TS (**2A-TS**) structures are depicted in Figure 1. In each structure, the cyclooctene moiety showed a twist conformation. In the **2A-TS**, the bonds (C \cdots O and CO \cdots C) to be broken were calculated to be 2.173 and 1.887 Å, respectively. The changes in bond lengths in the change of structure GS to TS are consistent with expectation as CO₂ breaks away. The decarboxylation mechanism belongs to the category of a $[2\pi+2\sigma+2\sigma]$ reaction.

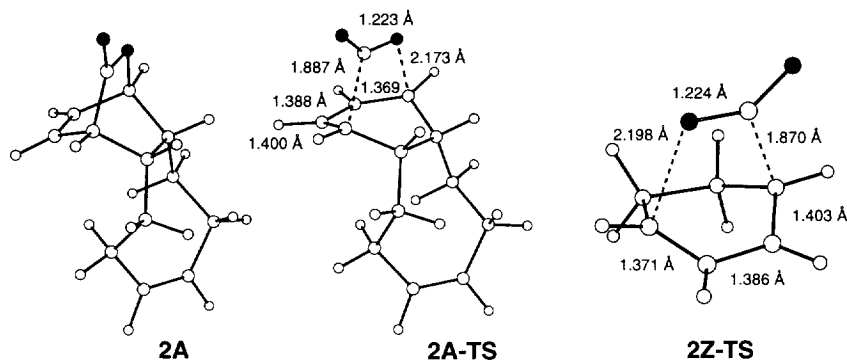


Figure 1. The 3-21G TS Structures (**2A-TS** and **2Z-TS**) for the Decarboxylation of the DDA Adducts (**2A** and **2Z**).

The 3-21G calculated reaction barrier is 52.5 kcal/mol. The 6-31G* and MP2/6-31G**/3-21G level calculations of the reaction barrier were beyond the capacity of Gaussian 92. Therefore, the decarboxylation reaction (**2Z** \rightarrow **2Z-TS**) of the DA adduct of 2-pyrone and ethylene was investigated. As shown in Table 1, the 3-21G calculation of the model reaction gave analogous value to that for **2A** \rightarrow **2A-TS**. The C \cdots O and CO \cdots C bonds were calculated to be 2.198 and 1.870 Å, respectively. The reaction barriers at the 6-31G**/3-21G and MP2/6-31G**/3-21G single-point levels are 49.9 and 37.7 kcal/mol, respectively.

So far as we know, there are few reports concerning to the MO calculation on the decarboxylation of the DA adduct of 2-pyrone and olefins.

Transition Structure of the IMDA Reaction

The 3-21G optimized GS of the decarboxylated DA adduct (**3A**) also takes a twisted conformation, in which the interacting C \cdots C distances between the diene and dienophile moieties are 3.159 and 4.190 Å. The 3-21G transition structure (**3A-TS**) of the IMDA reaction was calculated to be symmetrical (Figure 2). The reaction barrier (**3A** \rightarrow **3A-TS**) is 28.1 kcal/mol, comparable to the experimentally obtained value.⁷ The value is *ca.* 6 kcal/mol smaller than that for the open chain system (**3B** \rightarrow **3B-TS**, 34.1 kcal/mol), *i.e.*, the IMDA reaction of the decarboxylated DA adduct (**3B**) of 2-pyrone and 1,5-hexadiene. The high IMDA reactivity of the COD adduct is considered to be due to sterically favorable orbital interaction between the diene and dienophile moieties in the ground state.

It is noted that the PM3 calculated activation parameters ($\Delta H^\ddagger=26.4$ kcal/mol, $\Delta S^\ddagger=10.7$ e.u. at 300K) for the IMDA reaction of **3A** are close to the observed values.⁷

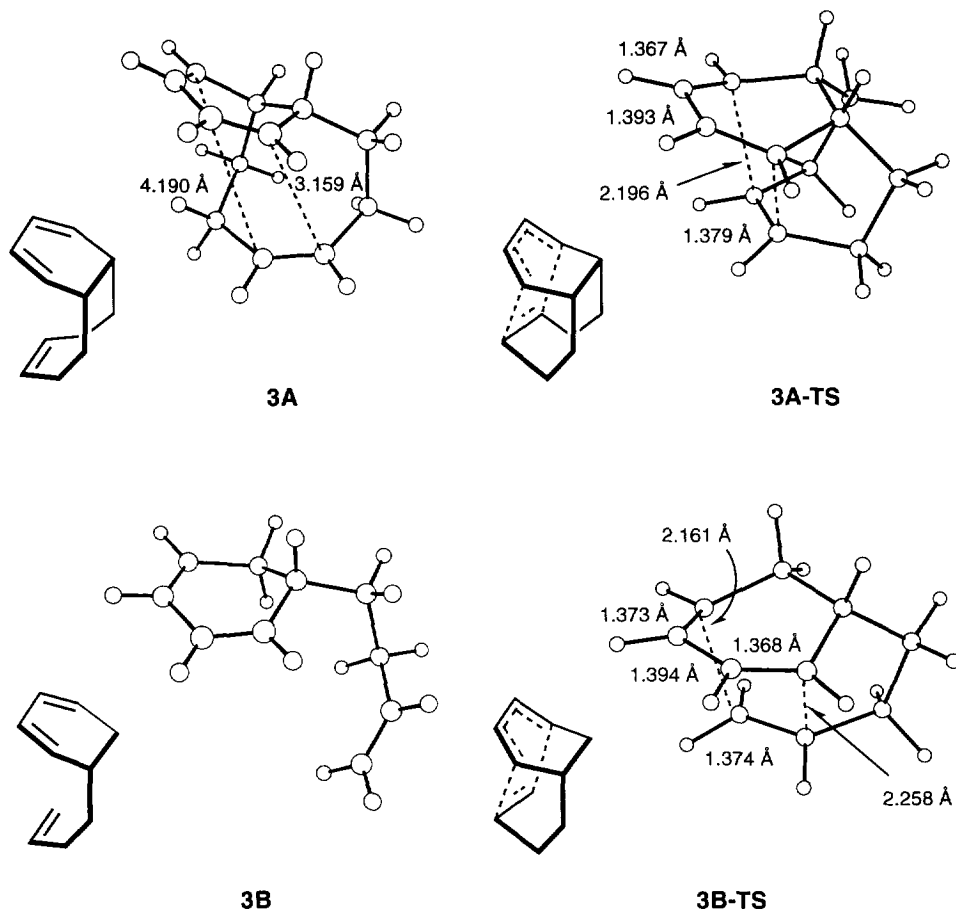
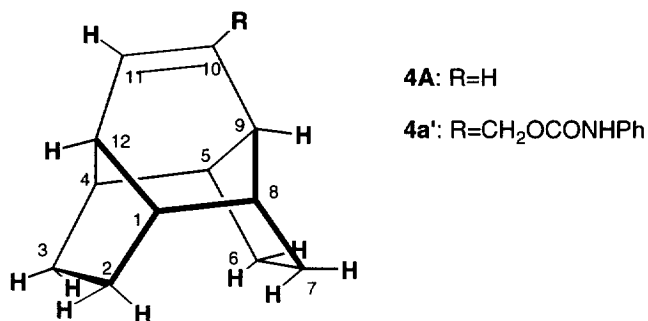


Figure 2. The 3-21G Transition Structures (**3A-TS** and **3B-TS**) for the IMDA Reactions of **3A** and **3B**.

Structure of the DDA Adduct

The single crystal X-ray structure of **4a'** showed very close C/C contacts (and H/H contacts) and short double bond. Semi-empirically derived values for the close C/C and H/H distances were considerably short. In order to obtain more accurate structural informations, the *ab initio* structure optimizations at several levels were carried out. The selected important structural data are summarized in Table 2 (see also Notes).⁸ For the *ab initio* calculation at 3-21G level, the close C/C contacts of **4A** is 2.914 Å, close to an average experimental value [2.910 (10) Å].^{2a} The calculation at MP2/6-31G level gave 2.957 Å, longer than the observed value. The MM3 value is 2.913 Å.

In all calculations, the bond length of C1-C8 was calculated to be considerably longer than the X-ray value (1.552(8) Å). The *ab initio* (3-21G) and MM3 values are 1.573 Å and 1.581 Å, respectively. The MP2/6-31G* calculation gave an improved value of 1.565 Å.

**Table 2.** Selected Atomic Distances for the Calculated Structures.

Method	-H ₂ C ² -----C ⁷ H ₂ -	>C ² -H ----- H-C ⁷ <	-HC ¹⁰ =C ¹¹ H-
X-ray ^{a)}	2.907(10)	1.890(85)	1.306(8)
	2.913(10)	1.982(85)	
RHF/STO-3G	2.938	1.975	1.308
RHF/3-21G	2.914	1.950	1.317
MP2/3-21G	2.926	1.929	1.348
RHF/6-31G	2.938	1.994	1.324
RHF/6-31G*	2.944	2.018	1.318
MP2/6-31G	2.957	1.980	1.358
MP2/6-31G*	2.924	1.976	1.343
MNDO	3.007	2.093	1.346
AM1	2.856	1.849	1.341
PM3	2.836	1.747	1.335
MM2	2.949	2.057	1.333
MM3	2.913	1.944	1.331

a) Data of **4a'**. See ref. 2a.

It seems reasonable that the hydrogen positions can be estimated from structures whose C/C contacts were well reproduced. Based on the 3-21G and MM3 calculated structures, we can safely say that the nonbonded H/H distance of **4A** is close to 1.950 Å.

Table 3 shows the *ab initio* calculation data for typical examples of the close C/C and H/H contacts. *Endo, endo*-tetracyclo[6.2.1.1^{3,6}.0^{2,7}]dodecane (**A**)⁹ has two short H/H contacts in the molecule. The 3-21G C/C distance (3.273 Å) is shorter by 0.025 Å than the X-ray value (see Table 3), whereas in *exo, exo*-tetracyclo[6.2.1.1^{3,6}.0^{2,7}]dodecane (**B**)⁹ the C/C distance is calculated to be longer by 0.021 Å than the neutron value.

MNDO calculation has been known to underestimate the nonbonding repulsion of hydrogen atoms. As far as close H/H contacts like **4** are concerned, the PM3 and AM1 calculations are considered to still underestimate the nonbonded H-H distance.^{3b}

Another structural feature of **4a'** is short double bond (1.306(8) Å),¹⁰ which is longer by 0.01 Å than the double-bond length (1.296 Å) of cyclopropene and comparable to allene (1.308 Å). The STO-3G distance (1.308 Å) is the closest and the 3-21G and 6-31G* values (1.317-1.318 Å) are longer by 0.011-0.012 Å than the observed one. The MP2 calculations at 3-21G, 6-31G and 6-31G* levels predicted normal double bond character (1.343-1.358 Å). However, the bond lengths from the RHF calculation are generally calculated to be shorter than the experimental values. At this stage, it is not clear whether the double bond can be well reproduced by the *ab initio* calculation. The MM3 bond length (1.331 Å) is 0.025 Å longer than the X-ray

value.

At first glance, the short double bond seemed to be arisen from the close C/C and H/H contacts. This view may be ruled out by the fact that the MM and MO calculations on a hypothetical DDA adduct having serious nonbonded interactions due to close Cl/Cl contacts did not affect the double bond length [1.335 (H) \rightarrow 1.328 Å (Cl) in MM3 and 1.335 (H) \rightarrow 1.332 Å (Cl) in PM3]. The $^1\text{H-NMR}$ spectrum showed the olefinic proton of the DDA adduct of 2-pyrone and COD resonates at 7.51 ppm which is at lower field than those of structurally similar alkenes (e.g., crotonic acid 7.10 ppm). The bond shortening is probably due to an increase of s character of the double bond whose π -orbitals interact with the strained σ -bonds of the adjacent atoms.

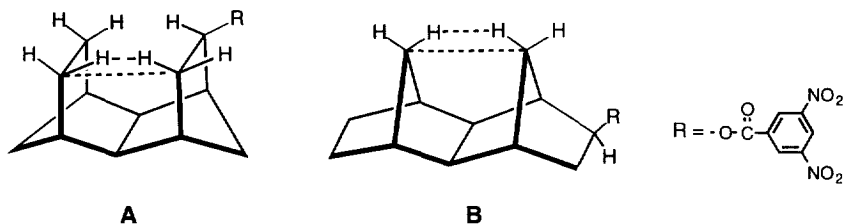


Table 3. C/C and H/H Distances for the Tetracyclo[6.2.1.1^{3,6}.0^{2,7}]dodecane derivatives.

Method		-HC-----CH-	>C-H ----- H-C<
Compound A			
	X-ray ^{a)}	3.298	1.85
	3-21G	3.273	1.837
	MM3	3.290	1.827
Compound B			
	Neutron ^{b)}	3.112	1.754 (4)
	3-21G	3.133	1.800
	MM3	3.124	1.751

a) Data of 3,5-dinitrobenzoate. See ref. 9a.

b) Data of 3,5-dinitrobenzoate. See ref. 9b.

Spectral Feature of the DDA Adducts

The close contacts of the hydrogen atoms reflects on their chemical shifts of the $^1\text{H-NMR}$ spectra. Figure 3 shows the $^1\text{H-}$ and $^{13}\text{C-NMR}$ spectral data of some DDA adducts derived from the pericyclic reactions of cyclopentadienone derivatives with COD. The assignment of the methylene proton signals was performed by comparison of the $^1\text{H-NMR}$ spectral data¹¹ of the DDA adduct (**4c**) of **1c** and COD with those of the DDA adduct (**4e**) of **1e** and COD. In **4e**, the outer protons (1.53-1.54 ppm) are shielded by the phenyl ring and the inner protons (1.93-1.96 ppm) are unaffected by the ring current effect. In **4c**, the methylene protons on C2, C3, C6 and C7 appeared as two groups (1.70-1.72 and 1.90-1.93 ppm). The inner protons of both the adducts (**4c** and **4e**) appeared beyond 1.90 ppm. The low-field shifted signals are ascribed to the inner protons. The DDA adduct (**4a**) of 2-pyrone and COD showed similar spectral feature. The inner protons appeared at 1.65-1.77 ppm and outer ones appeared at 1.46-1.54 ppm. The low-field shift of the hydrogen atoms is assumed to be due to steric compression.¹²

In the $^{13}\text{C-NMR}$ spectrum of the DDA adduct (**4b**), the upfield shift of methylene carbon (26.1, 25.7 ppm)

was observed in comparison with that of the DDA adduct (**4b**) of 2-pyrone and 1,5-hexadiene (32.1ppm). The high-field shift from the normal position may be due to the steric interference among the hydrogen atoms on C2(C3) and C7(C6).¹³

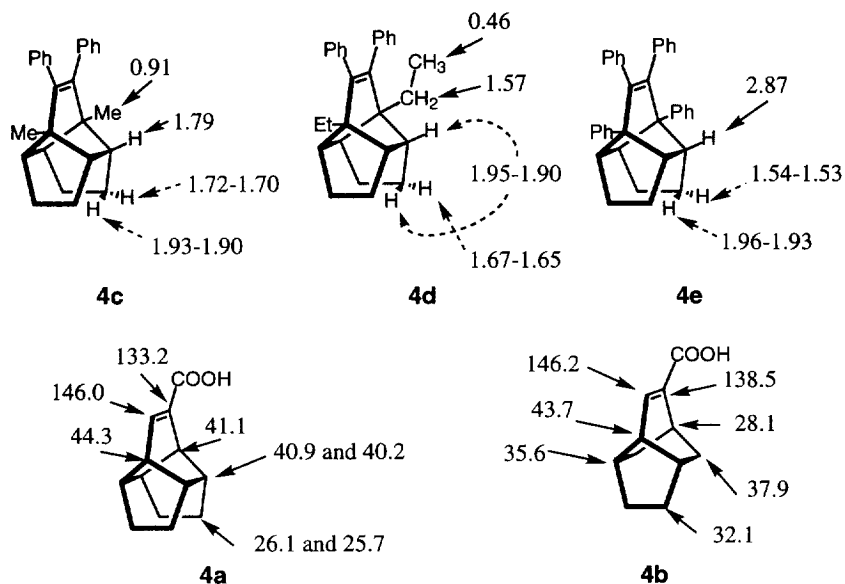


Figure 3. NMR Chemical Shifts (δ) of DDA Adducts

The 3-21G frequency calculation of the parent cage molecule **4A** predicts that the inner protons appear at a higher frequency region than the outer ones [inner; 3284.5 (intensity 21.5)–3334.3 (intensity 59.8) cm^{-1} , outer; 3214.4 (intensity 6.53)–3266.8 (intensity 124.4) cm^{-1}]. The commonly-used practice to scale down (by 0.92) the calculated frequencies to bring them into better accordance with experiment gave 2923.2–2967.3 and 2860.8–2916.1 cm^{-1} , respectively, supporting the observed spectral feature for the carboxylic acid derivative (**4a**) [2984 (inner), 2940, 2916 and 2880 (outer)].

In conclusion, the *ab initio* calculation at the 3-21G level is considered to give reliable mechanistic informations about the DDA formation reaction studied. The calculation also provides good agreement with experiment for the fine structure of the DDA adduct and afforded a clue to interpret the IR and NMR spectral changes arisen from the close C/C (H/H) contacts.

REFERENCES AND NOTES

1. K. H. Houk, Y. Li and J. D. Evanseck, *Angew. Chem. Int. Ed. Engl.*, **1992**, 31, 682.
2. a) M. Eto, K. Harano and T. Hisano, *J. Chem. Soc. Perkin Trans. 2*, **1993**, 963. b) M. Eto, T. Aoki and K. Harano, *Tetrahedron*, **1994**, 50, 13395. c) K. Harano, T. Aoki, M. Eto and T. Hisano, *Chem. Pharm. Bull.*, **1990**, 38, 1182. d) The single crystal X-ray analysis was performed on the phenylurethane (**4a'**) of the 10-hydroxymethyl derivative obtained from LiAlH_4 reduction of the DDA adduct (**4a**) of methyl coumalate and COD.
3. a) M. J. S. Dewar, E. G. Zoebisch, E. F. Healy and J. J. P. Stewart, *J. Am. Chem. Soc.*, **1985**, 107,

3902. b) J. J. P. Stewart, *J. Comp. Chem.*, **1989**, 10, 209; J. J. P. Stewart, *J. Comp. Chem.*, **1989**, 10, 221. c) AM1 and PM3 calculation are performed using MOPAC; J. J. P. Stewart, *QCPE Bull.*, **1989**, 9, 10. d) N. L. Allinger, Y. H. Yuh and J. -H. Lii, *J. Am. Chem. Soc.*, **1989**, 111, 8551; J. -H. Lii and N. L. Allinger, *J. Am. Chem. Soc.*, **1989**, 111, 8566, 8576; N. L. Allinger, F. Li and L. Yan, *J. Comp. Chem.*, **1990**, 11, 848.
4. a) H. F. Allen and J. A. Vanallan, *J. Am. Chem. Soc.*, **1950**, 72, 5165. b) H. F. Allen, *Chem. Rev.*, **1945**, 37, 209.
5. I. A. Akhtar, G. I. Fray and J. M. Yarrow, *J. Chem. Soc.(C)*, **1968**, 812.
6. Gaussian 92, Revision G.3, M. J. Frisch, G. W. Trucks, M. Head-Gordon, P. M. W. Gill, M. W. Wong, J. B. Foresman, B. G. Johnson, H. B. Schlegel, M. A. Robb, E. S. Replogle, R. Gomperts, J. L. Andres, K. Raghavachari, J. S. Binkley, C. Gonzalez, R. L. Martin, D. J. Fox, D. J. Defrees, J. Baker, J. J. P. Stewart, and J. A. Pople, *Gaussian Inc., Pittsburgh PA*, 1992.
7. The activation energy (ΔE_a) for the formation reaction of the DDA cycloadduct (**4A**) was 21.8 ± 0.25 kcal/mol.; W. Grimme and G. Wiechers, *Tetrahedron Lett.*, **1987**, 6035.
8. The X-ray and calculated bond lengths of **4a'** (**4A**) are listed below. The MP2/6-31G* calculation well reproduced the bond lengths except the double bond but is very time consuming.

distance	X-ray (4a')	3-21G (4A)	MP2/6-31G* (4A)	MM3 (4A)
C ¹ -C ²	1.539(8)	1.551	1.541	1.552
C ¹ -C ⁸	1.552(8)	1.573	1.565	1.581
C ¹ -C ¹²	1.556(8)	1.562	1.556	1.548
C ² -C ³	1.539(10)	1.568	1.554	1.558
C ¹⁰ -C ¹¹	1.306(8)	1.317	1.343	1.331
C ¹¹ -C ¹²	1.485(7)	1.494	1.485	1.511

9. a) O. Ermer, *Angew. Chem., Int. Ed. Engl.*, **1977**, 16, 798. b) O. Ermer and S. A. Mason, *J. Chem. Soc., Chem. Commun.*, **1983**, 53.
10. The *ab initio* calculations at RHF level seem to underestimate double bond lengths. The double bond lengths of typical olefinic compounds calculated by several MO methods are as follows:

	STO-3G	3-21G	6-31G*	MP2/6-31G*	AM1	PM3	MM3
Cyclopropene	1.277	1.282	1.276	1.303	1.318	1.314	1.314
Cyclobutene	1.314	1.326	1.322	1.347	1.354	1.349	1.354
Ethylene ^{a)}	1.306	1.315	1.317	1.336	1.354	1.349	1.337
Norbornene	1.311	1.319	1.321	1.346	1.344	1.339	1.341

- a) B3LYP/6-31G* 1.331Å.
11. In the ¹H-NMR spectrum of the DDA adduct (**4d**) of **1d** and COD, the methyl signal appeared at 0.46 ppm, considerably higher field than that of the DDA adduct (**4c**) of **1c** and COD. The NOESY spectrum of **4d** indicates the presence of the correlation between the phenyl and methyl protons. The PM3-optimized structure indicates that the ethyl moieties are placed in a very crowded circumstance and the methyl protons are forced to be located above the edge of the phenyl ring.
12. D. Lenoir and R. M. Frank, *Angew. Chem. Int. Ed. Engl.*, **1980**, 19, 318.
13. K. Tori, M. Ueyama, T. Tsuji, H. Matsumura and H. Tanida, *Tetrahedron Lett.*, **1974**, 327.